Ecotoxicology and Environmental Safety 179 (2019) 119–126

Contents lists available at ScienceDirect

Ecotoxicology and Environmental Safety

journal homepage: www.elsevier.com/locate/ecoenv

Acute exposure to triphenyl phosphate (TPhP) disturbs ocular development and muscular organization in zebrafish larvae

Qipeng Shi[a,b], Mirabelle M.P. Tsui[c], Chenyan Hu[d], James C.W. Lam[c,e], Bingsheng Zhou[a], Lianguo Chen[a,*]

[a] State Key Laboratory of Freshwater Ecology and Biotechnology, Institute of Hydrobiology, Chinese Academy of Sciences, Wuhan, 430072, China
[b] University of Chinese Academy of Sciences, Beijing, 100049, China
[c] State Key Laboratory in Marine Pollution, City University of Hong Kong, Tat Chee Avenue, Kowloon, Hong Kong, China
[d] School of Chemistry and Environmental Engineering, Wuhan Institute of Technology, Wuhan, 430072, China
[e] Department of Science and Environmental Studies, The Education University of Hong Kong, 10 Lo Ping Road, Tai Po, New Territories, Hong Kong, China

ARTICLE INFO

Keywords:
Triphenyl phosphate
Developmental toxicity
Proteomics
Phagosome
Visual development
Muscle contraction

ABSTRACT

Triphenyl phosphate (TPhP) is an organophosphate flame retardant that is frequently detected in the environments. TPhP exposure is known to cause developmental toxicity. However, the underlying molecular mechanisms remain underestimated. In the present study, zebrafish embryos were acutely exposed to 0, 4 and 100 μg/L TPhP until 144 h post-fertilization. Profiles of differentially expressed proteins were constructed using a shotgun proteomic. With the input of differential proteins, principal component analysis suggested different protein expression profiles for 4 and 100 μg/L TPhP. Gene ontology and KEGG pathway analyses further found that effects of TPhP at 4 μg/L targeted phagosome and lysosome activity, while 100 μg/L TPhP mainly affected carbohydrate metabolism, muscular contraction and phagosome. Based on proteomic data, diverse bioassays were employed to ascertain the effects of TPhP on specific proteins and pathways. At gene and protein levels, expressions of critical visual proteins were significantly changed by TPhP exposure, including retinoschisin 1a, opsins and crystallins, implying the impairment of ocular development and function. TPhP exposure at 100 μg/L also altered the abundances of diverse muscular proteins and disordered the assembly of muscle fibers. Effects of TPhP on visual development and motor activity may be combined to disturb larval swimming behavior. In summary, current results provided mechanistic clues to the developmental toxicities of TPhP. Future works are inspired to broaden the toxicological knowledge of TPhP based on current proteomic results.

1. Introduction

Since the ban on lower brominated flame retardants, alternative use of organophosphate esters has been gradually increasing (USEPA, 2005). Triphenyl phosphate (TPhP) is one of the primary organophosphate esters, being applied as flame retardants, plasticizers and anti-foaming agents in a variety of industries, including plastics, furniture, textile, electronics, construction, vehicle and petroleum industries (Van der Veen and de Boer, 2012; Wei et al., 2015). The production and use of TPhP within Western Europe is up to 20,000–30,000 tons in 2000 (Van der Veen and de Boer, 2012). Because TPhP additives can easily leak into the environment from applications (Lassen and Lokke, 1999), occurrences of TPhP have been ubiquitously detected in various environmental abiotic and biotic samples (Greaves and Letcher, 2017). For example, concentrations of TPhP range from several ng/L to tens of μg/L in river waters (Andresen et al., 2004; Lassen and Lokke, 1999; Green et al., 2007; Zha et al., 2018). TPhP has even been detected in drinking water from eight cities of China, which concentrations vary between 19.8 ng/L and 84.1 ng/L (Li et al., 2014). In sediment samples from the large river basin estuaries/deltas in Europe, TPhP can reach a concentration as high as 9553 pg/g (Wolschke et al., 2018). Furthermore, TPhP is hydrophobic and possesses the bioaccumulative capability in animals (Hou et al., 2016). Previous monitoring studies report that concentrations of TPhP reach 21 – 180 μg/kg lipid weight in perch from Swedish lakes and coastal areas (Sundkvist et al., 2010), and 280 μg/kg lipid weight in lake trout (*Salvelinus namaycush*) (Guo et al., 2017). Up to 45.7 μg/kg lipid weight of TPhP has also been reported in muscle samples of freshwater fishes from the Pearl River Delta region in South China (Ma et al., 2013; Y. Liu et al., 2018).

TPhP exposure can induce multiple toxic effects, including

* Corresponding author.
E-mail address: lchenam@ihb.ac.cn (L. Chen).

https://doi.org/10.1016/j.ecoenv.2019.04.056
Received 28 December 2018; Received in revised form 22 March 2019; Accepted 18 April 2019
Available online 28 April 2019
0147-6513/

neurotoxicity (Jarema et al., 2015; Noyes et al., 2015; Sun et al., 2016a; Hong et al., 2018), thyroid endocrine disruption (Kim et al., 2015; Liu et al., 2013a), reproductive impairment (Chen et al., 2015; Ding et al., 2017; Liu et al., 2013b) and cardiotoxicity (Du et al., 2015; McGee et al., 2013; Mitchell et al., 2018). Transcriptomic and metabolomic profiling in adult zebrafish show that TPhP exposure mainly affects carbohydrate metabolism, lipid metabolism and DNA damage repair system (Du et al., 2016). TPhP exposure also leads to developmental cardiac impairments in zebrafish larvae, which is speculatively mediated by retinoic acid receptor (Isales et al., 2015). Soubry et al. (2017) reports that urinary metabolites of TPhP are associated with increased DNA methylation aberrancies in sperm. After combined consideration of environmental occurrences, bioaccumulation and toxicities, TPhP exposure will pose a rising hazard to environmental and human health.

Although multiple toxicities have been reported for TPhP, molecular mechanisms underlying the developmental toxicity of TPhP are still underestimated. Therefore, the objectives of the present study were to elucidate the affected biological processes and reveal the mechanistic changes for TPhP's developmental toxicity by using high-throughput proteomic analyses. An acute exposure to 0, 4 and 100 μg/L TPhP was performed using zebrafish embryos (*Danio rerio*) until 144 h post-fertilization (hpf). Based on endpoints of developmental toxicities, a shotgun proteomic assay was employed here to profile the differentially expressed protein, aiming to provide preliminary insights into the toxic mechanisms of TPhP. Bioinformatic analyses of differential proteins further identified the concerning effects, which were verified by a suite of molecular assays at gene, protein and histological levels. Employment of proteomic profiling in this study can provide a comprehensive screening of developmental toxicity-related pathways, which will serve as inspiring clues for future targeted research.

2. Materials and methods

2.1. Chemicals

TPhP (CAS#115-86-6; > 99% purity), dimethyl sulfoxide (DMSO; CAS 67–68-5; ≥99.5% purity), methanesulfonate (MS-222), methionine, DL-homocysteine, sulfonylsalicylic acid and betaine were purchased from Sigma-Aldrich (St. Louis, MO, USA). Rabbit primary antibody to betaine-homocysteine S-methyltransferase (BHMT) was obtained from Abcam (Cambridge, UK). Mouse myosin heavy chain antibody (F59) was obtained from DSHB (University of Iowa, Iowa City, IA, USA). All other chemicals used in the present study were of analytical grade or high-performance liquid chromatography grade.

2.2. Zebrafish maintenance and embryo exposure

The culture of adult zebrafish (Wild type, AB strain, four-month-old) and embryo exposure were carried out as previously described (Chen et al., 2013). Briefly, 500 embryos that developed normally and reached the blastula stage (2 hpf) were randomly distributed in glass beakers, each of which contained 500 mL exposure solution with nominal concentrations of TPhP at 0, 4 and 100 μg/L. The choice of TPhP exposure concentrations was based on environmentally realistic concentrations (7.9 μg/L; Lassen and Lokke, 1999) and our previous toxicological observations (Shi et al., 2018), facilitating both ecological relevance and elucidation of toxicological mechanisms. All groups received equal amounts of DMSO (0.01% v/v). Actual waterborne concentrations of TPhP were measured at 4.4 and 109.2 μg/L, respectively, after the water renewal (Shi et al., 2018). Because the measured concentrations were close to nominal concentrations, current study used nominal concentrations as previous study did. There were 4 replicates for each group ($n = 4$). During exposure period, the solutions were renewed daily. Embryonic development was monitored and recorded every day, including survival, hatching and malformation (e.g., pericardial edema and axial spinal curvature). Zebrafish larvae at 144 hpf were fixed in 4% methyl cellulose to count heart beats within 1 min under stereomicroscope ($n = 20$). Body length of zebrafish larvae were also measured. After exposure until 144 hpf, the larvae were anesthetized using 0.03% MS-222 and randomly collected from exposure beakers for each separated bioassay, which were immediately frozen in liquid nitrogen and stored at −80 °C.

2.3. Proteomic profiling and bioinformatic analyses

A shot-gun proteomic experiment was conducted to profile the differentially expressed proteins in zebrafish larvae according to a previously published method (Chen et al., 2016a). Briefly, 300 larvae at 144 hpf were collected from each beaker of control, 4 and 100 μg/L groups ($n = 3$), and homogenized in lysis buffer (8 M urea and 40 mM HEPES, pH 7.4) on ice using a tissue tearer (BioSpec Products). The homogenates were subsequently sonicated vigorously on ice using a Misonix Sonicator-XL2020 (Misonix, NY, USA). After centrifugation, the supernatant was transferred and cleaned using methanol and chloroform to remove lipids, carbohydrates and salts (Wessel and Flügge, 1984). Protein pellets were then reconstituted in 100 μL of lysis buffer and quantified using a RC-DC assay kit (Bio-Rad, Hercules, CA, USA). An aliquot of 150 μg protein from each sample was separated by 12% SDS-PAGE electrophoresis. After staining by Coomassie brilliant blue, each lane of the gel was cut into three pieces according to the band density and the proteins were in-gel reduced, alkylated and digested. The resulting peptides were extracted and characterized on a Thermo Scientific LTQ Velos platform (Thermo Fisher Scientific, Bremen, Germany). Generated MS data were searched against the protein database of *D. rerio* on MASCOT platform (version 2.3, Matrix Sciences Ltd., London, UK) to determine the identity and quantity of each protein. Searching criteria were set as follows: trypsin specificity; two maximum missed cleavages; carbamidomethylation on cysteine and oxidation on methionine as variable modifications; peptide and fragment mass tolerance at 1.0 Da and 0.2 Da, respectively. Search results were merged for each sample. Cutoff of false discovery rate during MASCOT search was controlled at 1%.

Differentially expressed proteins were filtered using one-tailed Student's *t*-test or Mann Whitney *U* test according to following thresholds: detected in at least two replicates with spectral counts ≥5; fold change relative to control > 1.4, and $P < 0.05$ compared with the control group. Hierarchical clustering analysis with the input of differential proteins was performed using Gene Cluster 3.0 software, employing Spearman Rank Correlation for the calculation of similarity metric and centroid linkage as the cluster method. Gene ontology (GO) analysis was conducted using the g:GOSt module of a web server g:Profiler (Reimand et al., 2016). Statistically significant enrichment of GO terms (Biological process, Cellular component and Molecular function) was determined against the database of *D. rerio* ($P < 0.05$). Significantly represented pathways and diseases of differential proteins (Benjamini and Hochberg's corrected P value < 0.05) were annotated and identified on a web server KOBAS 3.0 using hypergeometric test and Fisher's exact test (Xie et al., 2011). Based on the list of differential proteins from all exposure groups, principal component analysis (PCA) was conducted according to the variance-covariance matrix in PAST software to observe the grouping and separation of samples on PCA plot.

2.4. Quantitative real-time polymerase chain reaction (qRT-PCR)

Isolation of total RNA, synthesis of first-strand cDNA and qRT-PCR assay were performed as previously described (Chen et al., 2012). Briefly, 30 zebrafish larvae were collected from each beaker ($n = 4$ per group) and homogenized to extract total RNA using Trizol reagent (Invitrogen Corp., Carlsbad, CA). Quality and purity of RNA extracts were assessed by 1% agarose-formaldehyde gel electrophoresis and measuring 260/280 nm ratio on a NanoDrop 2000 spectrophotometer

(Thermo Fisher Scientific). The first-strand cDNA was synthesized using a PrimeScript® RT Reagent Kit (Takara, Dalian, China). The qRT-PCR assay was carried out using SYBR® Real-time PCR Master Mix-Plus Kits (Toyobo, Osaka, Japan) and analyzed on an ABI 7300 system (PerkinElmer Applied Biosystems, Foster city, CA, USA). The primer sequences of opsin genes (*zfrho*, *zfred*, *zfgr1*, *zfuv* and *zfblue*) were obtained from previous research (Chen et al., 2013). The ribosomal protein L8 (*rpl8*) was selected as a reference gene, which transcription did not vary upon TPhP exposure (data not shown). We have verified the stability of *rpl8* by using geNorm software. List of primer pairs was provided in Table S1 of Supplementary materials. The transcriptional levels of opsin genes were normalized to that of *rpl8* using the $2^{-\Delta\Delta Ct}$ method.

2.5. Western blot assay

Abundances of BHMT proteins in zebrafish larvae were examined using Western blot assay as previously described (Chen et al., 2012). Approximately 100 larvae were collected for each replicate ($n = 4$ per group). Briefly, 50 μg of protein was separated by running on 12% SDS-PAGE, and then transferred to polyvinylidene difluoride membranes. The membranes were blocked with 5% fat-free milk for 2 h, and then probed with rabbit primary antibodies against BHMT (1: 1000) and GAPDH (1: 1000) at 4 °C overnight. After repeated washes, the blots were incubated with HRP-conjugated secondary antibody (1: 50,000) for 2 h at 37 °C, and then visualized by enhanced chemiluminescence. Relative optical density of each band was analyzed using Kodak film (Eastman Kodak Co., Rochester, NY) and Quantity One version 4.3 software (Bio-Rad, USA).

2.6. BHMT enzymatic activity

The enzymatic activity of BHMT in zebrafish larvae was measured according to descriptions in a previous study (Yagisawa et al., 2006). Briefly, 50 larvae from each beaker ($n = 4$) were homogenized in 500 μL of PBS buffer (pH 7.4) and then centrifuged at 12,000 × *g* at 4 °C for 10 min. An aliquot of 100-μl supernatant was mixed with 350 μl of 50 mM K-phosphate buffer (pH 7.3), 50 μl of 50 mM DL-homocysteine and 50 μl of betaine. The reaction mixture was incubated at 37 °C for 30 min. After cooling on ice, reaction was terminated by adding 500 μl of 0.15 M HCl. The reaction mixture was further filtered through 0.45 μm filters (Whatman) and subsequently examined by an automatic amino acid analyzer (Membrapure A300, Germany). Total protein concentration was measured by Bradford method. A unit of BHMT activity is defined as the amount of synthesized methionine per microgram protein per min.

2.7. Methionine content

Methionine concentrations in zebrafish larvae at 144 hpf were measured using an automatic amino acid analyzer (Membrapure A300, Germany). Approximately 50 larvae from each beaker ($n = 4$ per group) were homogenized in 300 μL of PBS buffer (pH 7.4) and centrifuged at 12,000 × *g* at 4 °C for 10 min. The supernatant were mixed with 20% sulfonylsalicylic acid for 15 min at room temperature, and then centrifuged at 14,000 × *g* at 4 °C for 30 min. The reaction mixture was filtered through 0.45 μm filters (Whatman) and subjected to an automatic amino acid analyzer to determine methionine concentrations (mg/g protein). Total protein concentration was measured by Bradford method.

2.8. Immunostaining of muscle fiber patterning

Alterations in muscle fiber assembly by TPhP exposure were examined by whole-fish immunostaining of zebrafish larvae at 144 hpf from the control and 100 μg/L exposure group (He et al., 2011). Six larvae were randomly collected from each replicate beaker ($n = 4$ per group). After anesthetized using 0.03% MS-222, larvae were fixed with 4% paraformaldehyde and decolorized in 10% H_2O_2 overnight. Subsequently, zebrafish larvae were washed, blocked with 1% Triton X-100 for at least 4 h, and incubated with primary mouse myosin heavy chain antibody (F59) overnight at 4 °C in 1% non-immune goat serum in PBST. After incubation with a DyLight488-conjugated secondary antibody (Abbkine, Redlands, CA, USA) for 1 h at room temperature, images of larval zebrafish were recorded using a laser scanning confocal microscope (Zeiss, LMS710, Jena, Germany).

2.9. Statistical analyses

All data were presented as means ± SEM of replicates. After initial verification of normal distribution and homogeneity of variance using the Kolmogorov–Smirnov and Levene's tests, respectively, significant differences between the control and exposure groups were evaluated by one-way analysis of variance (ANOVA), followed by the post-hoc LSD test. Unless specified (e.g., proteomic bioinformatics), all statistical analyses were performed using SPSS 18.0 software (IBM SPSS Statistics, IBM Corporation, Armonk, New York). Statistically significant difference is indicated by $P < 0.05$.

3. Results

3.1. Developmental toxicities

Acute TPhP exposure did not change the survival rate of zebrafish larvae (Table 1). However, larval hatching at 48 hpf was significantly delayed by 4 and 100 μg/L TPhP. This hatching delay continued at 72 hpf in 100 μg/L exposure group relative to the control (Table 1). A significant increase in malformation rate (1.5%) was observed after acute exposure to 100 μg/L TPhP compared to the control level at 0.3% (Table 1). The major malformation symptom was pericardial edema in exposed larvae. Furthermore, heat rate and body length of zebrafish larvae were significantly decreased in exposure groups compared to the control group (Table 1).

3.2. Proteomic profiling of differentially expressed proteins

Shotgun proteomics identified the profile of differential proteins in zebrafish larvae after 144-hpf exposure to 4 and 100 μg/L TPhP relative to the control expressions (Figs. S1 and S2). Among the list of differential proteins in 4 μg/L exposure group, 17 proteins had decreased abundances, while 28 proteins had increased abundances (Fig. 1A). In zebrafish larvae exposed to 100 μg/L TPhP, the number of differential proteins (133) was remarkably increased compared to that in 4 μg/L

Table 1
Developmental toxicities in zebrafish larvae after acute exposure to TPhP at 4 and 100 μg/L.[a].

TPhP (μg/L)		Control	4	100
Survival rate (%)[b]		93.8 ± 0.4	93.9 ± 0.6	92.9 ± 0.7
Hatching rate (%)[b]	48-hpf	16.0 ± 2.6	8.7 ± 0.8 *	5.4 ± 1.0 **
	72-hpf	95.2 ± 1.6	92.3 ± 2.0	87.6 ± 3.0 *
Malformation rate (%)[b]		0.3 ± 0.0	0.8 ± 0.4	1.5 ± 0.4 **
Heart rate (beats/min)[c]		169.9 ± 1.1	169.1 ± 3.6	160.3 ± 3.6 *
Body length (mm)[c]		3.0 ± 0.0	2.9 ± 0.0 **	2.8 ± 0.0***

[a] The asterisks denote significant differences in exposure groups compared with the control group: *$P < 0.05$, **$P < 0.01$ and ***$P < 0.001$.

[b] Values represent the mean ± SEM of four replicates; Survival rate % = numbers of living larvae/total numbers of embryos; Hatching rate % = numbers of hatched larvae/total numbers of embryos; Malformation rate % = numbers of malformed larvae/numbers of living embryos.

[c] Values represent the mean ± SEM of approximately twenty larvae.

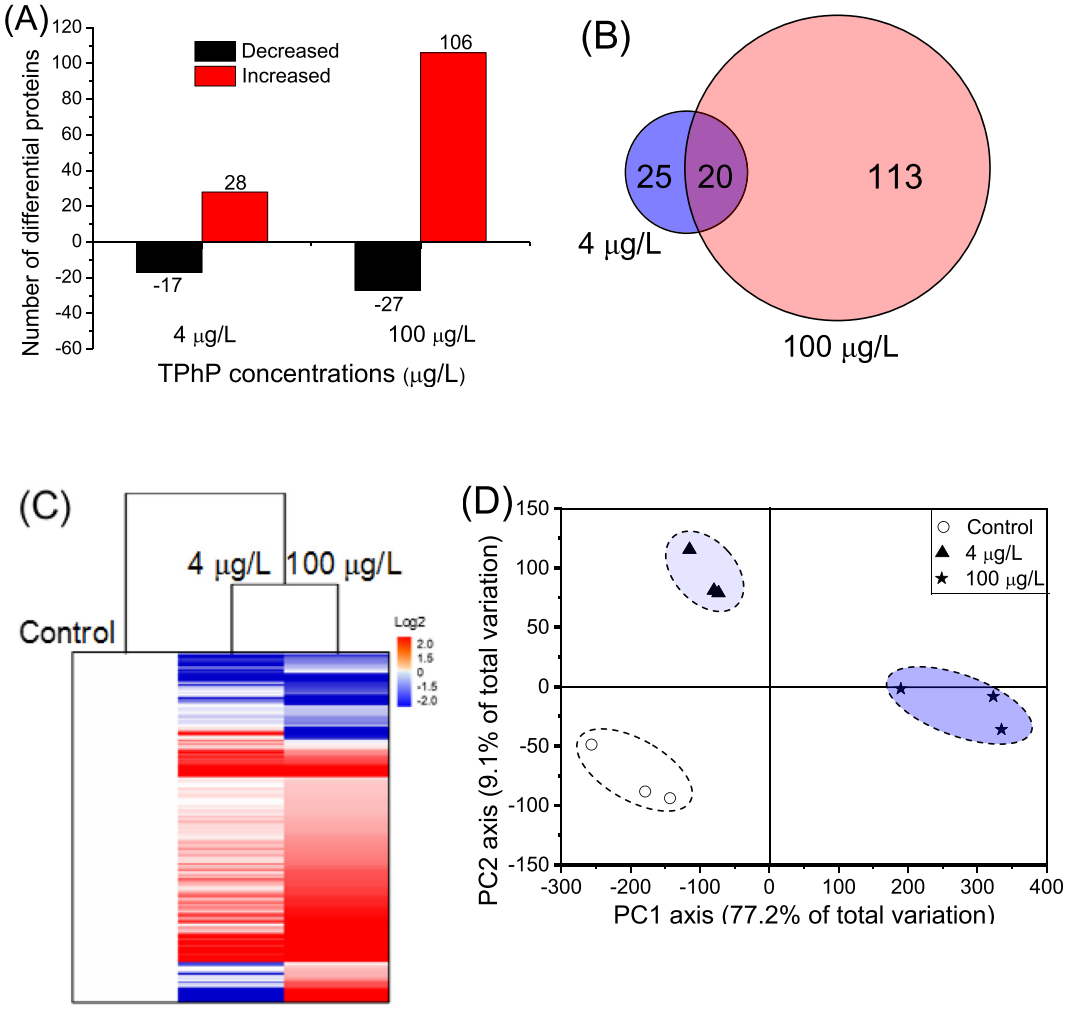

Fig. 1. Summary and analysis of differentially expressed proteins in zebrafish larvae after exposure to 4 and 100 μg/L TPhP until 144 hpf. (A) Number of differentially expressed proteins with increased or decreased abundances. **(B)** Venn diagram showing common and unique differential proteins in 4 and 100 μg/L exposure groups. **(C)** A heatmap showing the overall distribution of differential proteins; Red coloring indicates up-regulation and blue coloring indicates down-regulation; Color intensity is proportional to the magnitude of changes. **(D)** PCA plot based on differential proteins; Samples of control, 4 and 100 μg/L groups are separately grouped along PC1 and PC2 axes. (For interpretation of the references to color in this figure legend, the reader is referred to the Web version of this article.)

exposure group (45). Majority of differential proteins in 100 μg/L group were up-regulated in expressions (106 up-regulated proteins and 27 down-regulated proteins). A venn diagram demonstrated the overlapped and specific proteins in 4 and 100 μg/L TPhP exposure groups (Fig. 1B). It was found that each exposure group (4 μg/L or 100 μg/L) possessed a large part of specific differential proteins, especially in 100 μg/L TPhP group. Heatmap also showed that 4 and 100 μg/L groups had a distinct profile of differential proteins (Fig. 1C). Based on the profiles of differentially expressed proteins, PCA plot grouped and separated samples of control, 4 and 100 μg/L groups (Fig. 1D). PC1 axis explained 77.2% of total variation, while PC2 axis explained 9.1% of total variation. Each exposure group was separated clearly on PCA plot, implying their different toxic mechanisms.

GO analysis annotated the significantly overrepresented terms in biological process (BP), cellular component (CC) and molecular function (MF) for each exposure group (Table S2 in Supplementary materials). In 4 μg/L exposure group, effects of TPhP concentrated on primary lysosome (i.e., dense body) and affected the enzymatic activities, including hydrolase, pyrophosphatase, nucleoside-triphosphatase and ATPase (Table S2). In 100 μg/L exposure group, much more biological processes were affected by TPhP acute exposure, especially for muscle contraction, carbohydrate metabolism and primary lysosome activities (Table S2).

KEGG pathway analysis showed that differential proteins in 4 μg/L exposure group were predominantly enriched in biological processes about phagosome ($P < 0.001$) and Salmonella infection ($P < 0.001$; Fig. S3). In zebrafish larvae exposed to 100 μg/L TPhP, top 10 processes of significant enrichment were phagosome ($P < 0.001$), tight junction ($P < 0.001$), regulation of actin cytoskeleton ($P < 0.001$), carbon metabolism ($P < 0.001$), oocyte meiosis ($P < 0.001$), biosynthesis of amino acids ($P < 0.001$), protein processing in endoplasmic reticulum ($P < 0.001$), ribosome ($P = 0.001$), Salmonella infection ($P = 0.002$) and adrenergic signaling in cardiomyocytes ($P = 0.003$; Fig. S3).

3.3. Disturbances in visual development

Proteomic analysis identified several critical visual proteins of differential abundances in zebrafish larvae after TPhP exposure (Fig. 2A), including retinoschisin 1a, rhodopsin and two crystallin proteins (crystalline, beta B1 and crystallin, beta B1, like 1). Retinoschisin 1a had a significantly decreased abundance in 4 μg/L exposure group, while rhodopsin expression was significantly decreased by 100 μg/L

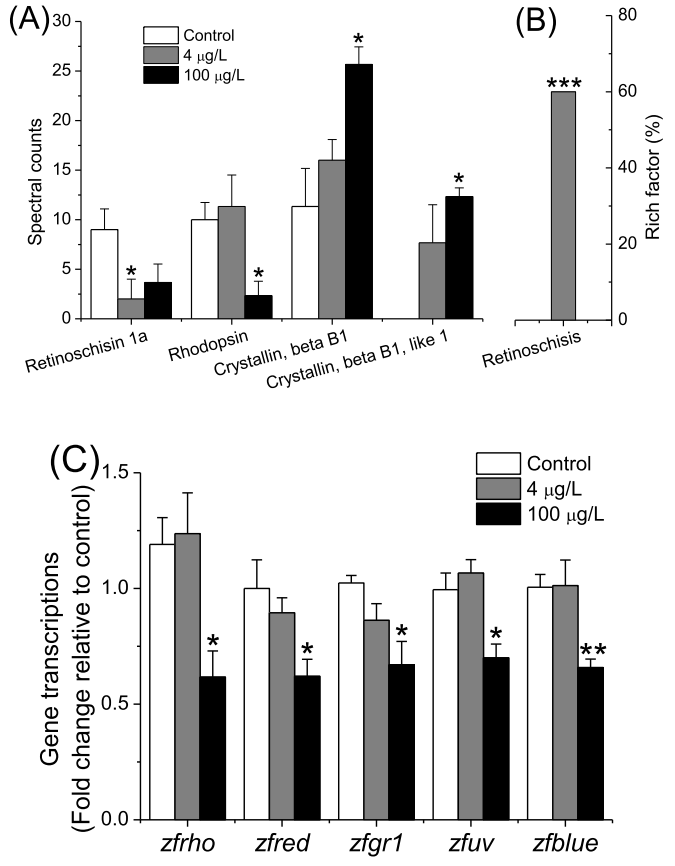

Fig. 2. Disturbances in visual development in zebrafish larvae after exposure to 4 and 100 μg/L TPhP until 144 hpf. (A) Proteomic analysis identifies visual proteins of differential abundances. **(B)** Overrepresentation of retinoschisis disease in larvae from 4 μg/L exposure group. **(C)** Alterations in gene transcriptions of opsins (*zfrho*, *zfred*, *zfgr1*, *zfuv* and *zfblue*). Significant differences between exposure and control groups are indicated by $*P < 0.05$, $**P < 0.01$ and $***P < 0.001$.

TPhP. Two crystalline proteins were significantly up-regulated in zebrafish larvae from 100 μg/L exposure group. Human Phenotype Ontology of g:Profiler server found significant enrichment in an eye disease, namely retinoschisis ($P < 0.001$), by retinoschisin 1a, actin, cytoplasmic 1 and actin, cytoplasmic 2 (Fig. 2B).

Transcriptional levels of five opsin genes were also examined by qRT-PCR tests in exposed zebrafish larvae (Fig. 2C). Similar to decreased protein abundances of rhodopsin, transcriptions of *zfrho*, *zfred*, *zfgr1*, *zfuv* and *zfblue* genes, which encode rhodopsin, red, green, ultraviolet and blue opsins, respectively, were significantly and consistently down-regulated to 0.6-, 0.6-, 0.7-, 0.7- and 0.7-fold in the 100 μg/L group relative to the control.

3.4. Alterations in BHMT activity

According to proteomic results, protein abundances of BHMT 1 (A0A2R8PWR1 and Q32LQ4) were significantly up-regulated in 4 and 100 μg/L exposure groups compared to the control group (Fig. 3A), which was further verified by Western blot assay of BHMT (Fig. 3A and B).

In contrast to increase in protein abundances, enzymatic activity of BHMT protein was significantly inhibited by 16.4% in zebrafish larvae exposed to 100 μg/L TPhP relative to that in the control larvae (Fig. 4A). Consequently, total concentration of methionine, which is the synthesis product of BHMT, was also remarkably lowered by 69.7% in zebrafish larvae from 100 μg/L exposure group in comparison with the

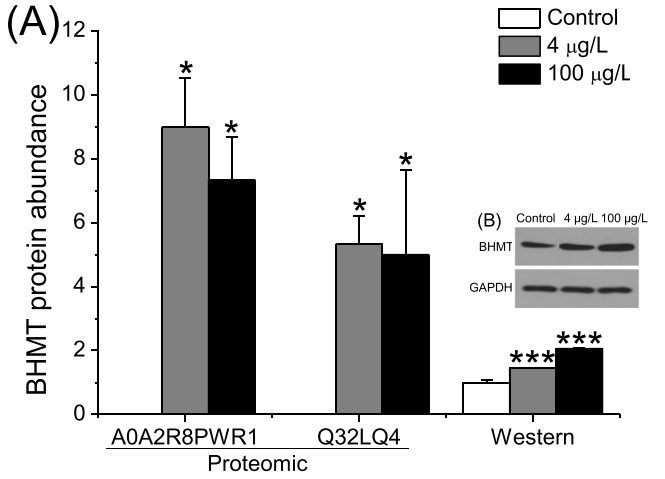

Fig. 3. Alterations in BHMT protein expressions in zebrafish larvae after exposure to 4 and 100 μg/L TPhP until 144 hpf. (A) Proteomic and Western blot analysis show increased abundances of BHMT proteins. **(B)** Representative graph of Western blot against BHMT protein with GAPDH as a reference. Significant differences between exposure and control groups are indicated by $*P < 0.05$ and $***P < 0.001$.

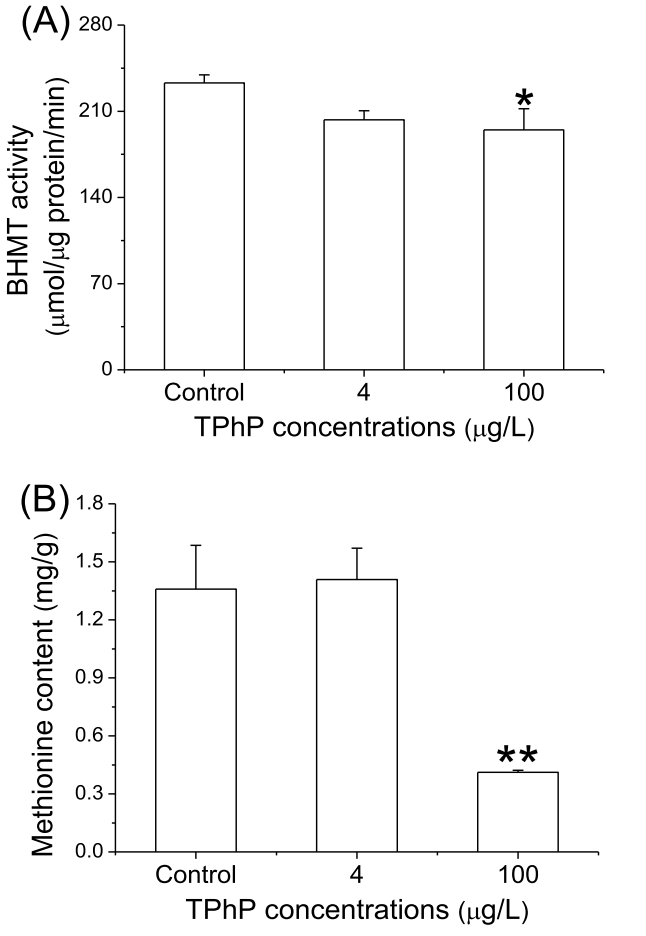

Fig. 4. Disturbances in BHMT-mediated process in zebrafish larvae after exposure to 4 and 100 μg/L TPhP until 144 hpf. (A) BMHT enzymatic activity. **(B)** Methionine content. Significant differences between exposure and control groups are indicated by $*P < 0.05$ and $**P < 0.01$.

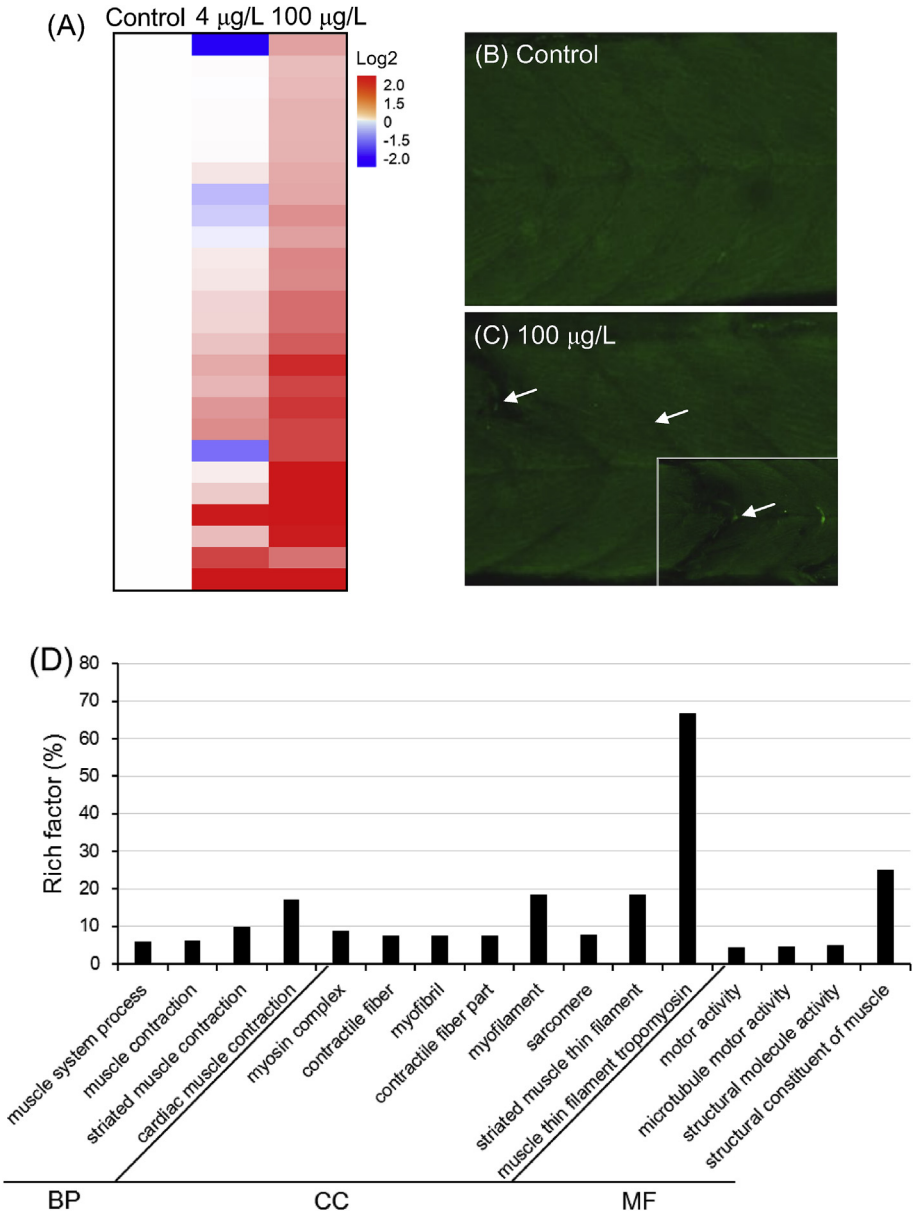

Fig. 5. Disorganization of muscular assembly in zebrafish larvae after exposure to 4 and 100 μg/L TPhP until 144 hpf. (A) A heatmap showing the overall distribution of muscular proteins of differential abundances; Red coloring indicates up-regulation and blue coloring indicates down-regulation; Color intensity is proportional to the magnitude of changes. **(B and C)** Staining of myofibril pattern showing the loosely packed and ruptured fibers (arrows) in zebrafish larvae from 100 μg/L exposure group. **(D)** Significantly enriched GO terms associated with muscle development and function in 100 μg/L exposure group (BP, Biological process; CC, Cellular component; MF, Molecular function); Rich factor (%) is calculated by dividing mapped query protein against total background protein in each term. (For interpretation of the references to color in this figure legend, the reader is referred to the Web version of this article.)

control level (Fig. 4B).

3.5. Disorganized pattern of muscular fiber

Heatmap clustering showed that expression profile of diverse muscular proteins was dramatically modified in zebrafish larvae of 100 μg/L group, being significantly consistently up-regulated (Fig. 5A). Compared to the control larvae (Fig. 5B), immunostaining of myosin observed a disorganized assembly of muscle fibers in larvae from 100 μg/L exposure group, as characterized by loosely packed fibers and ruptured fibers (Fig. 5C). Furthermore, GO enrichment of differential proteins found that muscle organization and contraction activity of zebrafish larvae were significantly affected by 100 μg/L TPhP (Fig. 5D).

4. Discussion

Employing a shotgun proteomic assay, the present study investigated the molecular mechanisms underlying acute developmental toxicities of TPhP in zebrafish larvae. According to the list of differentially expressed proteins, bioinformatic analyses found that TPhP at low and high exposure concentrations (i.e., 4 and 100 μg/L) affected distinct biological processes in the induction of embryonic anomalies. TPhP at 4 μg/L targeted primary lysosome (i.e., dense body) and affected the enzymatic activities, while high concentration of TPhP at 100 μg/L mainly affected muscle contraction, carbohydrate metabolism and primary lysosome activities. At gene and protein levels, TPhP acute exposure significantly changed the expressions of critical ocular proteins, which play important roles in the maintenance of visual functions. Consistent with protein expression profile, assembly of muscular fibers was disordered by 100 μg/L TPhP. In zebrafish larvae exposed to 100 μg/L TPhP, biosynthesis of amino acids was significantly altered, as verified by differential protein abundances and enzyme activity of BHMT as well as decreased methionine content. By combining developmental endpoints, proteomic profiling and other bioassays (e.g., qRT-PCR, Western blot, enzyme activity and immunostaining), current study is expected to provide mechanistic clues in the developmental toxicities of TPhP.

TPhP at both low and high exposure concentrations significantly affected the phagosome and lysosome activities in zebrafish larvae. A previous transcriptomic study also find significant enrichment in

phagosome in liver tissues of adult zebrafish after 7 days exposure to 0.05 mg/L and 0.3 mg/L TPhP (Du et al., 2016). Acute exposure to TPhP also induced the infection of Salmonella bacteria, certain species of which are intracellular pathogens (Jantsch et al., 2011). Normally, phagocytes will engulf pathogens to form phagosome, which will fuse with lysosome to degrade pathogens by hydrolytic enzymes (Aderem, 2003). Because phagocytosis and lysosomal activities are crucial to prevent harms from pathogenic bacteria, targeted effects of TPhP on phagosome and lysosome may place the organisms under a higher risk of bacterial infection.

It is increasingly realized that ocular development and function are sensitive targets of environmental pollutants, which can accumulate in the eyes (Chen et al., 2018), change the expressions of critical visual proteins (Chen et al., 2013), disorganize retinal structure (Carvalho and Tillitt, 2004; W. Liu et al., 2018) and disturb visually-mediated behavior (Sun et al., 2016b; Xu et al., 2017). In this study, TPhP acute exposure is also found to disrupt the expressions of visual proteins in zebrafish larvae. Expression of retinoschisin 1a was significantly down-regulated by 4 μg/L TPhP. Retinoschisin protein plays an important role in the maintenance of retinal structure by facilitating cell adhesion (Vijayasarathy et al., 2012). Mutation of retinoschisin will cause degeneration of retinal macula and lead to a loss of vision (Kotova et al., 2010). Furthermore, decreased abundance of retinoschisin in zebrafish larvae was associated with retinoschisis disease, which symptom is characterized by abnormal splitting of retinal neurosensory layers (Cassin and Solomon, 1990). TPhP at 100 μg/L decreased opsin expressions, but increased the abundances of crystallins in current exposure. Previous toxicological studies also find inverse changes in opsin and crystallin expressions by environmental pollutants, which are characterized by decreased expression of opsins (Zhang et al., 2015), but increased abundances of crystallins (Chen et al., 2016b and 2017). Opsin proteins are synthesized in cone and rod photoreceptor cells and determine the spectral specificity of visual pigments (Vihtelic et al., 1999). Crystallins are integral structural components of eyes to regulate the transparency and function of lens and cornea (Jester, 2008). Therefore, abnormal expressions of opsin and crystallin proteins should be tightly involved in the impairment of ocular development and function by toxic pollutants. The opposite changing direction of opsins and crystallins may imply a self-adaptive response to increase light perception after photoreceptor impairment. Considering the sensitivity and importance, opsin and crystallin can be used as indicators of visual toxicity.

In addition, acute exposure to 100 μg/L TPhP significantly disturbed carbohydrate metabolisms in larval zebrafish. Disturbances in carbohydrate metabolism and TCA cycles are speculated as general effects of TPhP on cell metabolism (Alam et al., 2012; Scanlan et al., 2015; Du et al., 2016), which may result in deficiency of energy supply for cellular activities, especially for muscle contraction of high energy demand. Expression of multiple muscular proteins and assembly of muscle fibers were also disordered after TPhP exposure, thus affecting motor activity of zebrafish larvae. Lethargic swimming is previously observed in TPhP-exposed larvae of zebrafish (Shi et al., 2018), which is likely caused by the combined effects of visual reception, neural transmission, muscular contraction and energy supply. Additionally, TPhP exposure also significantly decreased the rate of heart beats in larval zebrafish. Our proteomic analysis found that TPhP developmental exposure caused interference with cardiac muscle contraction and adrenergic signaling in cardiomyocytes, which may be the responsible cause of impaired heart functions (Lohse et al., 2003).

5. Conclusions

In summary, the present study identified the expression profile of differential proteins in zebrafish larvae after acute exposure to 4 and 100 μg/L TPhP. The results showed that low and high concentrations of TPhP posed toxic effects via affecting different biological pathways. TPhP at 4 μg/L targeted lysosome activity and caused Salmonella infection, while TPhP at 100 μg/L mainly affected carbohydrate metabolism, muscular contraction and lysosome. Expressions of critical visual proteins were significantly changed by TPhP, implying impaired development and function of eyes. TPhP exposure at 100 μg/L also disturbed the abundances of muscular proteins, disordered the myofibril pattern and affected muscle contraction. Toxic effects on visual perception, neural signaling and muscle contraction may be combined to induce abnormal swimming, which will impact individual survival and population sustainability in wild. Results of current study are expected to provide mechanistic clues for future research, targeting specific proteins and pathways.

Conflicts of interest

The authors have no competing interests to declare.

Acknowledgements

This work was supported by the National Natural Science Foundation of China (grant number 21737005), the Strategic Priority Research Program of the Chinese Academy of Sciences (grant number XDB14040103), the State Key Laboratory of Freshwater Ecology and Biotechnology (grant number 2016FBZ11).

Appendix A. Supplementary data

Supplementary data to this article can be found online at https://doi.org/10.1016/j.ecoenv.2019.04.056.

References

Aderem, A., 2003. Phagocytosis and the inflammatory response. J. Infect. Dis. 187, S340–S345.
Alam, T.M., Neerathilingam, M., Alam, M.K., Volk, D.E., Ansari, G.A.S., Sarkar, S., Luxon, B.A., 2012. ^{1}H nuclear magnetic resonance (NMR) metabolomic study of chronic organophosphate exposure in rats. Metabolites 2, 479–495.
Andresen, J., Grundmann, A., Bester, K., 2004. Organophosphorus flame retardants and plasticisers in surface waters. Sci. Total Environ. 332, 155–166.
Carvalho, P.S.M., Tillitt, D.E., 2004. 2,3,7,8-TCDD effects on visual structure and function in swim-up rainbow trout. Environ. Sci. Technol. 38, 6300–6306.
Cassin, B., Solomon, S., 1990. Dictionary of Eye Terminology. Triad Publishing Company, Gainesville, Florida.
Chen, L., Huang, C., Hu, C., Yu, K., Yang, L., Zhou, B., 2012. Acute Exposure to DE-71: effects on locomotor behavior and developmental neurotoxicity in zebrafish larvae. Environ. Toxicol. Chem. 31, 2338–2344.
Chen, L., Huang, Y., Huang, C., Hu, B., Hu, C., Zhou, B., 2013. Acute exposure to DE-71 causes alterations in visual behavior in zebrafish larvae. Environ. Toxicol. Chem. 32, 1370–1375.
Chen, G., Zhang, S., Jin, Y., Wu, Y., Liu, L., Qian, H., Fu, Z., 2015. TPP and TCEP induce oxidative stress and alter steroidogenesis in TM3 Leydig cells. Reprod. Toxicol. 57, 100–110.
Chen, L., Zhang, W., Ye, R., Hu, C., Wang, Q., Seemann, F., Au, D.W.T., Zhou, B., Giesy, J.P., Qian, P.Y., 2016a. Chronic exposure of marine medaka (Oryzias melastigma) to 4,5-dichloro-2-n-octyl-4-isothiazolin-3- one (DCOIT) reveals its mechanism of action in endocrine disruption via the hypothalamus-pituitarygonadal-liver (HPGL) axis. Environ. Sci. Technol. 50, 4492–4501.
Chen, L., Zhu, B., Guo, Y., Xu, T., Lee, J.S., Qian, P.Y., Zhou, B., 2016b. High-throughput transcriptome sequencing reveals the combined effects of key e-waste contaminants, decabromodiphenyl ether (BDE-209) and lead, in zebrafish larvae. Environ. Pollut. 214, 324–333.
Chen, L., Wang, X., Zhang, X., Lam, P.K.S., Guo, Y., Lam, J.C.W., Zhou, B., 2017. Transgenerational endocrine disruption and neurotoxicity in zebrafish larvae after parental exposure to binary mixtures of decabromodiphenyl ether (BDE-209) and lead. Environ. Pollut. 230, 96–106.
Chen, L., Tsui, M.M.P., Shi, Q., Hu, C., Wang, Q., Zhou, B., Lam, P.K.S., Lam, J.C.W., 2018. Accumulation of perfluorobutane sulfonate (PFBS) and impairment of visual function in the eyes of marine medaka after a life-cycle exposure. Aquat. Toxicol. 201, 1–10.
Ding, K.K., Kong, X.T., Wang, J.P., Lu, L.P., Zhou, W.F., Zhan, T.J., Zhang, C.L., Zhuang, S.L., 2017. Side chains of parabens modulate antiandrogenic activity: *In vitro* and molecular docking studies. Environ. Sci. Technol. 51, 6452–6460.
Du, Z., Wang, G., Gao, S., Wang, Z., 2015. Aryl organophosphate flame retardants induced cardiotoxicity during zebrafish embryogenesis: by disturbing expression of the transcriptional regulators. Aquat. Toxicol. 161, 25–32.
Du, Z., Zhang, Y., Wang, G., Peng, J., Wang, Z., Gao, S., 2016. TPhP exposure disturbs

carbohydrate metabolism, lipid metabolism, and the DNA damage repair system in zebrafish liver. Sci. Rep. 6, 21827.
Greaves, A.K., Letcher, R.J., 2017. A review of organophosphate esters in the environment from biological effects to distribution and fate. Bull. Environ. Contam. Toxicol. 98, 2–7.
Green, N., Schlabach, M., Bakke, T., Brevik, E.M., Dye, C., Herzke, D., Huber, S., Plosz, B., Remberger, M., Schoyen, M., Uggerud, H.T., Vogelsang, C., 2007. Screening of Selected Metals and New Organic Contaminants. Norwegian Pollution Control Agency.
Guo, J.H., Venier, M., Salamova, A., Hiets, R.A., 2017. Bioaccumulation of dechloranes, organophosphate esters, and other flame retardants in Great Lakes fish. Sci. Total Environ. 583, 1–9.
He, J., Yang, D., Wang, C., Liu, W., Liao, J., Xu, T., Bai, C., Chen, J., Lin, K., Huang, C., Dong, Q., 2011. Chronic zebrafish low dose decabrominated diphenyl ether (BDE-209) exposure affected parental gonad development and locomotion in F1 offspring. Ecotoxicology 20, 1813–1822.
Hong, X., Chen, R., Hou, R., Yuan, L., Zha, J., 2018. Triphenyl phosphate (TPHP)-induced neurotoxicity in adult male Chinese Rare Minnows (*Gobiocypris rarus*). Environ. Sci. Technol. 52, 11895–11903.
Hou, R., Xu, Y., Wang, Z., 2016. Review of OPFRs in animals and humans: absorption, bioaccumulation, metabolism, and internal exposure research. Chemosphere 153, 78–90.
Isales, G.M., Hipszer, R.A., Raftery, T.D., Chen, A., Stapleton, H.M., Volz, D.C., 2015. Triphenyl phosphate-induced developmental toxicity in zebrafish: potential role of the retinoic acid receptor. Aquat. Toxicol. 161, 221–230.
Jantsch, J., Chikkaballi, D., Hensel, M., 2011. Cellular aspects of immunity to intracellular *Salmonella enterica*. Immunol. Rev. 240, 185–195.
Jarema, K.A., Hunter, D.L., Shaffer, R.M., Behl, M., Padilla, S., 2015. Acute and developmental behavioral effects of flame retardants and related chemicals in zebrafish. Neurotoxicol. Teratol. 52, 194–209.
Jester, J.V., 2008. Corneal crystallins and the development of cellular transparency. Semin. Cell Dev. Biol. 19, 82–93.
Kim, S., Jung, J., Lee, I., Jung, D., Youn, H., Choi, K., 2015. Thyroid disruption by triphenyl phosphate, an organophosphate flame retardant, in zebrafish (*Danio rerio*) embryos/larvae, and in GH3 and FRTL-5 cell lines. Aquat. Toxicol. 160, 188–196.
Kotova, S., Vijayasarathy, C., Dimitriadis, E.K., Ikonomou, L., Jaffe, H., Sieving, P.A., 2010. Retinoschisin (RS1) interacts with negatively charged lipid bilayers in the presence of Ca^{2+}: an atomic force microscopy study. Biochemistry 49, 7023–7032.
Lassen, C., Lokke, S., 1999. Danish Environmental Protection Agency (EPA), Brominated flame retardants: substance flow analysis and assessment of alternatives. DK EPA Report No. 494.
Li, J., Yu, N., Zhang, B., Jin, L., Li, M., Hu, M., Zhang, X., Wei, S., Yu, H., 2014. Occurrence of organophosphate flame retardants in drinking water from China. Water Res. 54, 53–61.
Liu, C., Wang, Q., Liang, K., Liu, J., Zhou, B., Zhang, X., Liu, H., Giesy, J.P., Yu, H., 2013a. Effects of tris(1,3-dichloro-2-propyl) phosphate and triphenyl phosphate on receptor-associated mRNA expression in zebrafish embryos/larvae. Aquat. Toxicol. 128–129, 147–157.
Liu, X., Ji, K., Jo, A., Moon, H.B., Choi, K., 2013b. Effects of TDCPP or TPP on gene transcriptions and hormones of HPG axis, and their consequences on reproduction in adult zebrafish (*Danio rerio*). Aquat. Toxicol. 134–135, 104–111.
Liu, W., Zhang, X., Wei, P., Tian, H., Wang, W., Ru, S., 2018. Long-term exposure to bisphenol S damages the visual system and reduces the tracking capability of male zebrafish (*Danio rerio*). J. Appl. Toxicol. 38, 248–258.
Liu, Y., Huang, L., Luo, X., Tan, X., Huang, C., Corella, P.Z., Mai, B., 2018. Determination of organophosphorus flame retardants in fish by freezing-lipid precipitation, solid-phase extraction and gas chromatography-mass spectrometry. J. Chromatogr. A 1532, 68–73.
Lohse, M.J., Engelhardt, S., Eschenhagen, T., 2003. What is the role of β-adrenergic signaling in heart failure? Circ. Res. 93, 896–906.
Ma, Y.Q., Cui, K.Y., Zeng, F., Wen, J.X., Liu, H., Zhu, F., Ouyang, G.F., Luan, T.G., Zeng, Z.X., 2013. Microwave-assisted extraction combined with gel permeation chromatography and silica gel cleanup followed by gas chromatography-mass spectrometry for the determination of organophosphorus flame retardants and plasticizers in biological samples. Anal. Chim. Acta 786, 47–53.
McGee, S.P., Konstantinov, A., Stapleton, H.M., Volz, D.C., 2013. Aryl phosphate esters within a major PentaBDE replacement product induce cardiotoxicity in developing zebrafish embryos: potential role of the aryl hydrocarbon receptor. Toxicol. Sci. 142, 445–454.
Mitchell, C.A., Dasgupta, S., Zhang, S., Stapleton, H.M., Volz, D.C., 2018. Disruption of nuclear receptor signaling alters triphenyl phosphate-induced cardiotoxicity in zebrafish embryos. Toxicol. Sci. 163, 307–318.
Noyes, P.D., Haggard, D.E., Gonnerman, G.D., Tanguay, R.L., 2015. Advanced morphological-behavioral test platform reveals neurodevelopmental defects in embryonic zebrafish exposed to comprehensive suite of halogenated and organophosphate flame retardants. Toxicol. Sci. 145, 177–195.
Reimand, J., Arak, T., Adler, P., Kolberg, L., Reisberg, S., Peterson, H., Vilo, J., 2016. g: profiler-a web server for functional interpretation of gene lists (2016 update). Nucleic Acids Res. 44, W83–W89.
Scanlan, L.D., Loguinov, A.V., Teng, Q., Antczak, P., Dailey, K.P., Nowinski, D.T., Kornbluh, J., Lin, X.X., Lachenauer, E., Arai, A., Douglas, N.K., Falciani, F., Stapleton, H.M., Vulpe, C.D., 2015. Gene transcription, metabolite and lipid profiling in eco-indicator daphnia magna indicate diverse mechanisms of toxicity by legacy and emerging flame-retardants. Environ. Sci. Technol. 49, 7400–7410.
Shi, Q., Wang, M., Shi, F., Yang, L., Guo, Y., Feng, C., Liu, J., Zhou, B., 2018. Developmental neurotoxicity of triphenyl phosphate in zebrafish larvae. Aquat. Toxicol. 203, 80–87.
Soubry, A., Hoyo, C., Butt, C.M., Fieuws, S., Price, T.M., Murphy, S.K., Stapleton, H.M., 2017. Human exposure to flame-retardants is associated with aberrant DNA methylation at imprinted genes in sperm. Environ. Epiqenet. 14, 1–13.
Sun, L., Tan, H., Peng, T., Wang, S., Xu, W., Qian, H., Jin, Y., Fu, Z., 2016a. Developmental neurotoxicity of organophosphate flame retardants in early life stages of Japanese medaka (*Oryzias latipes*). Environ. Toxicol. Chem. 35, 2931–2940.
Sun, J., Tang, S., Peng, H., Saunders, D.M.V., Doering, J.A., Hecker, M., Jones, P.D., Giesy, J.P., Wiseman, S., 2016b. Combined transcriptomic and proteomic approach to identify toxicity pathways in early life stages of Japanese medaka (*Oryzias latipes*) exposed to 1,2,5,6-tetrabromocyclooctane (TBCO). Environ. Sci. Technol. 50, 7781–7790.
Sundkvist, A.M., Olofssona, U., Haglunda, P., 2010. Organophosphorus flame retardants and plasticizers in marine and fresh water biota and in human milk. J. Environ. Monit. 12, 943–951.
USEPA, 2005. Furniture Flame Retardancy Partnership: Environmetnal Profiles of Chemical Flame-Retardant Alternatives for Low-Density Polyurethane Foam. Design for the Environment, Washington DC.
Van der Veen, I., de Boer, J., 2012. Phosphorus flame retardants: properties, production, environmental occurrence, toxicity and analysis. Chemosphere 88, 1119–1153.
Vihtelic, T.S., Doro, C.J., Hyde, D.R., 1999. Cloning and characterization of six zebrafish photoreceptor opsin cDNAs and immunolocalization of their corresponding proteins. Vis. Neurosci. 16, 571–585.
Vijayasarathy, C., Ziccardi, L., Sieving, P.A., 2012. Biology of retinoschisin. Adv. Exp. Med. Biol. 723, 513–518.
Wei, G., Li, D., Zhuo, M., Liao, Y., Xie, Z., Guo, T., Li, J., Zhang, S., Liang, Z., 2015. Organophosphorus flame retardants and plasticizers: sources, occurrence, toxicity and human exposure. Environ. Pollut. 196, 29–46.
Wessel, D., Flügge, U.I., 1984. A method for the quantitative recovery of protein in dilute solution in the presence of detergents and lipids. Anal. Biochem. 138, 141–143.
Wolschke, H., Sühring, R., Massei, R., Tang, J., Ebinghaus, R., 2018. Regional variations of organophosphorus flame retardants-Fingerprint of large river basin estuaries/deltas in Europe compared with China. Environ. Pollut. 236, 391–395.
Xie, C., Mao, X., Huang, J., Ding, Y., Wu, J., Dong, S., Kong, L., Gao, G., Li, C., Wei, L., 2011. KOBAS 2.0: a web server for annotation and identification of enriched pathways and diseases. Nucleic Acids Res. 39, W316–W322.
Xu, T., Liu, Y., Pan, R., Zhang, B., Yin, D., Zhao, J., Zhao, Q., 2017. Vision, color vision, and visually guided behavior: the novel toxicological targets of 2,2′,4,4′-tetrabromodiphenyl ether (BDE-47). Environ. Sci. Technol. Lett. 4, 132–136.
Yagisawa, M., Shigematsu, N., Nakata, R., 2006. Effects of chronic betaine ingestion on methionine-loading induced plasma homocysteine elevation in rats. J. Nutr. Sci. Vitaminol. 52, 194–199.
Zha, D., Li, Y., Yang, C., Yao, C., 2018. Assessment of organophosphate flame retardants in surface water and sediment from a freshwater environment (Yangtze River, China). Environ. Monit. Assess. 15, 190–222.
Zhang, X., Hong, Q., Yang, L., Zhang, M., Guo, X., Chi, X., Tong, M., 2015. PCB_{1254} exposure contributes to the abnormalities of optomotor responses and influence of the photoreceptor cell development in zebrafish larvae. Ecotoxicol. Environ. Saf. 118, 133–138.